



# XRD, DTA, DTG, XRF and TG Analysis of Developed Submerged Arc Welding Fluxes

<sup>1</sup>Aditya Kumar, <sup>2</sup>Sachin Maheshwari

Department of MPAE, Netaji Subhas Institute of Technology, Dwarka, New Delhi-110078, India.  
Email: <sup>1</sup>aditya\_rathihere@yahoo.com, <sup>2</sup>ssaacchhiinn@gmail.com

[Received: 18<sup>th</sup> Feb. 2017; Revised 27<sup>th</sup> Feb. 2017; Accepted: 28<sup>th</sup> Feb. 2017]

**Abstract** --- A study on chemicals and structural characterization of fluxes for SAW was carried out. All fluxes were designed by using a mixture of oxide, halide, carbonate, silicate by agglomeration process. Taguchi L 9 orthogonal array was used to design all the fluxes. One commercial flux was also used for comparison. All the fluxes were analysed by XRD to determine the different types of oxides formed as well as the change in oxidation number of constituents. To study the effect of temperature with phase transformation, DTA was carried out at 1000-1400 °C. This kind of study helps us in quantifying the ions that might be present in the plasma arc of SAW and also the melting behaviour of the developed fluxes for SAW. The analysis also helps in predicting the reaction in weld pool. XRF analysis will provide the chemical composition of the compound present with their weight percentage. TG analysis was performed to know the weight loss occurred during welding process.

**Key Words:** Agglomerated flux, DTA, DTG, Submerged arc welding, TG, XRD

## I. INTRODUCTION

Submerged arc welding (SAW) is a common arc welding process that requires a continuously fed consumable solid or tubular (metal cored) electrode. The thick layer of flux completely covers the molten metal thus preventing spatter and sparks as well as suppressing the intense ultraviolet radiation and fumes. It's mainly used for carbon steels (structural and vessel construction), low alloy steels, stainless steels, Nickel-based alloys and corrosion resistant overlay of steels. There are four ways to design the SAW fluxes. These are named fused flux, agglomerated flux, bonded flux and mechanical fluxes. SAW fluxes are manufactured fused at temperature exceeding 1400 °C, agglomerated from 400-900 °C<sup>1</sup>. Agglomeration is used for preparing flux by mixtures of oxides, halides, carbonates, silicate and Ferro-alloys<sup>2</sup>. The chemistry of weld metal is governed by electrochemical reactions happening at the weld pool. The most important characteristics of SAW are a function of fluxes and their physiochemical properties<sup>2-6</sup>. Major reactions taking place during firing of ceramic oxides are formation of a metal, reaction among different phases<sup>7,8</sup>, formation of crystalline phases<sup>9</sup>, characterization of crystalline phases in fluxes

<sup>10</sup> and phase transformation of minerals. Agglomerated fluxes are studied by the chemical analysis of crystalline phases during rise of temperature as phase transformation of crystalline phases predominate early stages of heating before the melt is formed. Formation of melt can be observed at a temperature as low as 920 °C because of the presence of impurities like earth oxides alkalis<sup>11</sup>. All this enables us to quantify the types of ions present and predict their behaviour when they are dissociated in a SAW process<sup>3</sup>. The objective of this study is to find the crystalline phases and crystal system present in the designed flux as well as to know the weight loss occurring during the process by using XRD and DTA and TG techniques.

## II. EXPERIMENTAL

### Selection of main flux constituents

The melting point of mild steel is approximately 1410 °C. In the Ternary phase diagram of CaO-Al<sub>2</sub>O<sub>3</sub>-SiO<sub>2</sub> a point at 1350 °C was selected. This point on the ternary phase diagram was selected, because the constituents of flux must melt well before the parent metal. This will also serve the purpose of the atmospheric contamination; the melted flux would remain in liquid state even after the solidification of weld metal to protect the heat loss from weld pool.

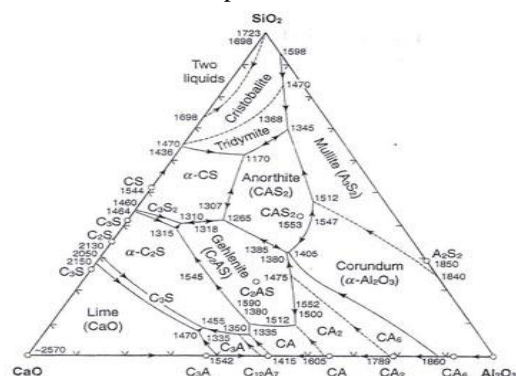


Figure 1 Actual Ternary phase diagram of CaO-Al<sub>2</sub>O<sub>3</sub>-SiO<sub>2</sub> flux system

### Flux composition

From this point the selection of three main components of flux can be calculated as shown below in Figure 2.

## Flux constituents level

Quantity of three main components such as CaO, SiO<sub>2</sub> and Al<sub>2</sub>O<sub>3</sub> are based on the position of the point in the ternary phase diagram. Three constituents such as NiO, MnO and MgO were selected as the additive. These were selected because of their function to improve the mechanical and other related properties of the weld zone. MgO increases the basicity of the slag that will prevent the oxygen content in the weld metal and also increases the refractiveness of the flux.

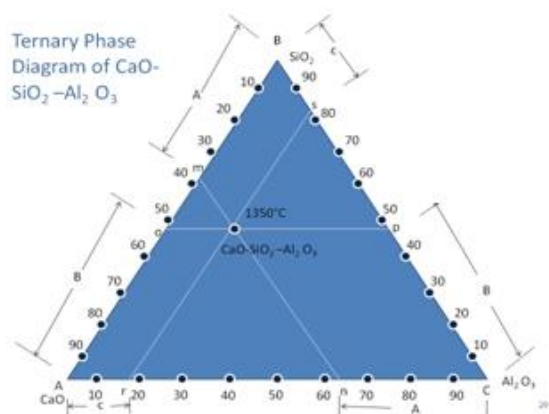


Figure 2 Ternary phase diagram for CaO-Al<sub>2</sub>O<sub>3</sub>-SiO<sub>2</sub>

MnO in the flux improves the toughness of weld metal; increase in the oxygen content in weld metal makes it tougher to remove the slag form the plate. Al<sub>2</sub>O<sub>3</sub> and Cr<sub>2</sub>O<sub>3</sub> will decrease arc stability. MnO, FeO, NiO, CaO, and TiO<sub>2</sub> are expected to have little effect on arc stability since their elemental ionization potentials are similar to that of iron. Their levels were decided by the composition of flux design. L 9 Orthogonal array was used to design the flux.

 Design of SiO<sub>2</sub> based flux:

In the ternary phase diagram as shown in Figure 2, three lines are drawn parallel to AB, BC and CA passing through 1350°C point. These lines will intersect the lines AB, BC and CA at various points located as mn, qp and rs in a ratio. The length of these lines such as nc for CaO, pc for SiO<sub>2</sub> and sb for Al<sub>2</sub>O<sub>3</sub> were measured. In Figure 2 A represents CaO, B represents SiO<sub>2</sub> and C represents Al<sub>2</sub>O<sub>3</sub>. These length ratios were converted into the composition of flux constituents. The main constituents of flux were taken as 70% and three additive were taken as 30%. Their levels are shown in Table 1 and 2 respectively.

Table 1 Composition of SiO<sub>2</sub> based flux

Constituents	Al <sub>2</sub> O <sub>3</sub>	SiO <sub>2</sub>	CaO	NiO
Wt % in gm	297	560	543	60-100
Constituents	MnO	MgO	CaF <sub>2</sub>	K <sub>2</sub> SiO <sub>2</sub>
Wt % in gm	50-90	85-105	150	2:1 ratio

Each constituent was weighed, mixed in a big container for 30 minutes and subsequently the binder potassium silicate was sprayed in the mixture after heating it at

50°C. The ratio of potassium silicate and water has been taken as 2:1. 10 mm steel balls were used to agglomerate the mixture thoroughly. The mixture was dried at room temperature for 48 hours after agglomeration process. All the fluxes were baked in a muffle furnace at 600°C before packing in an air tight container. A commercial welding flux was also used for comparison.

## III.RESULTS AND DISCUSSION

XRD analysis was performed in a diffractometer with monochromatic light of wavelength 1.540600 Å [Cu Kα] for

Table 2 Design matrix

S. No.	NiO	MnO	MgO
111	60	50	85
122	60	70	95
133	60	90	105
212	80	50	95
223	80	70	105
231	80	90	85
313	100	50	105
321	100	70	85
332	100	90	95

all the samples. It was performed in the following condition with 2θ - Start: 10.000 ° - End: 89.998 ° - Step: 0.019 ° - Step time: 38.4 s - Temp.: 25 °C (Room) - Time Started: 11 s - 2-Theta: 10.000 ° - Theta: 5.000 ° - Chi: 0.00 ° - Phi: 0. It can be observed by these graphs that a number of crystalline phases are formed due to the chemical reaction among ions with potassium silicate. The oxides such as CaCO<sub>3</sub>, SiO<sub>2</sub> and Al<sub>2</sub>O<sub>3</sub> were found in compound form, which means they do not react with one another. The development of different types of silicate and oxides is due to mixing of potassium silicate during the agglomeration process. The XRD analysis results of the developed agglomerated fluxes are depicted in Figures 1, 2, and 3 for first two fluxes and a commercial flux, data for the rest of the fluxes along with crystal structure and crystal system is presented in Table 3.

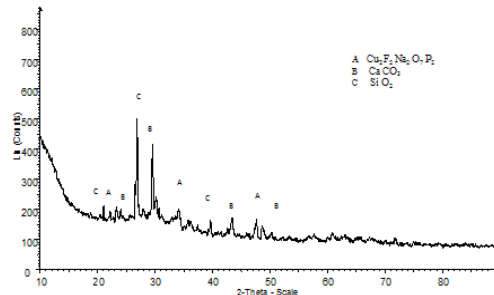


Figure 3 XRD Analysis of Flux 1

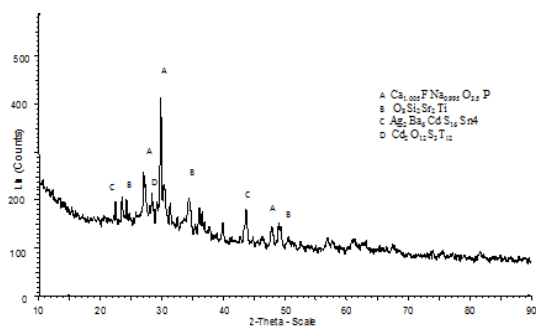


Figure 4 XRD Analysis of Flux 2

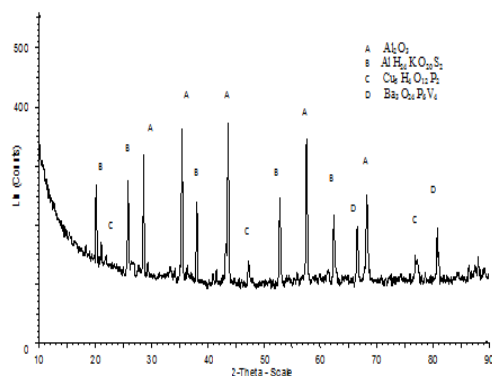


Figure 5 XRD Analysis of Commercial flux

Table 3 Crystalline Phase of Elements of flux present in XRD analysis

Type of flux	Crystalline Phase of Elements of flux
Flux 1 A B C	$\text{Cu}_2 \text{F}_2 \text{Na}_2 \text{O}_7 \text{P}_2$ (monoclinic), C Ca $\text{O}_3$ Calcite (trigonal (hexagonal axes)), $\text{O}_2 \text{Si}$ Quartz (trigonal (hexagonal axes))
Flux 2 A B C D	$\text{Ca}_{1.005} \text{FNa}_{0.995} \text{O}_{3.5} \text{P}$ (Cuspidine) (monoclinic), $\text{O}_8 \text{Si}_2 \text{Sr}_2 \text{Ti}$ (Strontium fresnoite) (tetragonal) $\text{Ag}_2 \text{Ba}_6 \text{CdS}_{16} \text{Sn}_4$ (cubic), $\text{Cd}_2 \text{O}_{12} \text{S}_3 \text{T}_{12}$ (cubic)
Flux 3 A B	Al $\text{Be}_3 \text{Ca}_4 \text{H}_3 \text{O}_{28}$ $\text{Si}_9$ (Bavenite) (orthorhombic), $\text{O}_8 \text{Si}_2 \text{Sr}_2 \text{Ti}$ (Strontium fresnoite) (Tetragonal)
Flux 4 A B C D	Al $\text{Be}_3 \text{Ca}_4 \text{H}_3 \text{O}_{28} \text{Si}_9$ (Bavenite) (orthorhombic), C Ca $\text{O}_3$ Calcite (trigonal (hexagonal axes)), $\text{CuF}_3 \text{KAl}_3 \text{Ba}_3 \text{P}_5$
Flux 5 A B C D	C Ca $\text{O}_3$ (Calcite) (trigonal (hexagonal axes)), $\text{O}_2 \text{Si}$ (Silicon oxide) trigonal (hexagonal axes), $\text{B}_6 \text{Sr}$ (SrB6) (cubic), $\text{B}_2 \text{Ti}_{0.5} \text{Zr}_{0.5}$ (hexagonal)
Flux 6 A B C	$\text{K}_2 \text{MnO}_{12} \text{V}_4$ (potassium manganese(II) polyvanadate) (monoclinic), C $\text{Ca}_{0.936} \text{Mg}_{0.0643}$ (Calcite) (trigonal (hexagonal axes)), $\text{Ba}_{3.97} \text{Fe}_3 \text{K}_{1.03} \text{O}_9$ (cubic)
Flux 7 A B C	$\text{Ca}_{9.8} \text{Fe}_{0.2} \text{K}_{0.8} \text{O}_{28} \text{P}_7$ (potassium decacalcium iron heptaphosphate) (

	trigonal (hexagonal axes)) C Ca $\text{O}_3$ Calcite) (trigonal (hexagonal axes)), $\text{Cr}_2 \text{P}$ (Chromium phosphide (2/1)) (orthorhombic)
Flux 8 A B C D E	$\text{CaO}_3 \text{S}$ (Wollastonite-2M) (monoclinic), $\text{Ca}_{1.25} \text{O}_4 \text{P Sr}_{0.25}$ (trigonal (hexagonal axes)) $\text{Cu}_2 \text{H}_4 \text{Na}_2 \text{O}_{13} \text{Si}_4$ (triclinic (anorthic)), $\text{C}_{16} \text{Co Fe H}_{18} \text{N}_6$ (cubic), $\text{Fe}_2 \text{MgO}_4$ (Magnesioferrite) (cubic)
Flux 9 A B C D	$\text{Al}_2 \text{O}_3$ (Corundum) (trigonal (hexagonal axes)), B $\text{H}_6 \text{K Mn O}_{11} \text{P}_2$ (hexagonal axes) $\text{Ba}_3 \text{O}_{24} \text{P}_6 \text{V}_4$ (cubic), $\text{Cu}_{1.25} \text{Fe}_{0.25} \text{S}$ (Bornite) (cubic)
Flux 10 A B C D	$\text{Al}_2 \text{O}_3$ (Aluminium oxide Corundum) (rhombohedral), Al $\text{H}_{24} \text{K O}_{20} \text{S}_2$ (Potassium aluminium bis (sulfate(VI) dodecahydrate Potassium Al) (cubic), $\text{Cu}_5 \text{H}_4 \text{O}_{12} \text{P}_2$ (Ludjibaite) triclinic (anorthic)) $\text{Ba}_3 \text{O}_{24} \text{P}_6 \text{V}_4$ (cubic)

The common elements detected by the XRD Analysis are Calcite, Corundum, Quartz, Strontium fresnoite and Bavenite. The crystal system for the most of the compounds is Cubic, Trigonal (hexagonal axes), monoclinic, orthorhombic and Triclinic in some of the cases.

#### DTA Analysis

Differential thermal analysis of flux was performed in Alumina crucible from 32 Celsius to 1400<sup>0</sup> Celsius at a heating rate of 10 Celsius / min. Alumina powder was used as a standard reference for DTA analysis. It was performed with sample weight of 10.75 mg and reference weight of 1.5 mg. Differential thermal analysis represents the temperature difference on y-axis with respect to temperature on x-axis. The DTA is destructive testing. It observes the change on state of the sample by heating or cooling of the sample. In DTA analysis, changes made are associated with change in enthalpy and heat capacity of the system. The temperature deviation is represented by  $\Delta T = T_S - T_R$ , where  $T_S$  = Temperature of sample and  $T_R$  = Temperature of reference point. This change in temperature is caused by consumption of heat in endothermic reaction and production of heat in exothermic reaction. The same is compensated by increased heat flux or decreased heat flux.

The curves of differential thermal analysis (DTA) for flux 1 and commercial flux are shown in Figures 7 and 8. The results of other fluxes are shown in Table 4. It is clear that most of the oxides were found to be stable up to 700<sup>0</sup> Celsius. There is a slight variation in the endothermic peaks of different

Table 4 DTA peak temperature and energy of SiO<sub>2</sub> flux

Type of flux	SiO <sub>2</sub> Flux	
	DTA Peak temp., Celsius	Energy (mJ/mg) , uv
111	693	37.6,-1.25
122	694	65.4,-1.39
133	697	30.9,-1.47
212	690	31.2,-1.32
223	695	16.5,-3.29
231	703	33.4,-5.74
313	696	31.9,-2.66

fluxes because of their chemical compositions. This can be related with the melting reaction of different crystalline phases for different fluxes. In some DTA curves, a zigzag curve shows gassing or blistering of the glass formation.

#### DTG Analysis

DTA, TG and DTG analysis were performed at IIT Roorkee test centre for SiO<sub>2</sub> based flux. Differential thermo gravimetric analysis gives an idea of weight loss compared with a standard sample in a controlled atmosphere. This analysis gives an idea of moisture present in the sample, thermal stability and weight loss occurring during the analysis.

The result of the analysis is shown in (Figure 7, 8) for flux 1 and commercial flux. Table 5 represents the result of analysis of all the fluxes compared with the commercial flux. Moisture is present in flux 5 and flux 9 as detected by the analysis at early stage otherwise all are stable up to 700 Celsius.

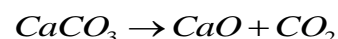
 Table 5 DTG peak temperature and loss of weight of SiO<sub>2</sub> flux

Type Of Flux	DTG SiO <sub>2</sub> Flux				
	First peak, Celsius	loss of weight, ug	second peak, Celsius	Loss of weight, ug	Third peak, Celsius
111			686	48	
122			700	65	
133			691	57	
212			685	53	
223	223	12	690	53	
231			694	77	
313			684	56	
321			692	78	
332	258	13	666	17	
Co. flux	88	15	262	8	1037

#### TG Analysis

Figure 6 and 7 represent the comparison of flux 1 and commercial flux for all the three analysis. Table 6 clearly represents the data of TG analysis of the flux. It is clear from this table that all the flux losses weight up to 600 Celsius and after wards the deoxidation takes due to the release of CO<sub>2</sub> occurs at around 715 Celsius. Then

the oxidation takes place for all the fluxes system. It means that the flux is reacting with the atmosphere. The observation is made up to 1397 Celsius.



#### XRF Analysis of flux:

To know the elemental composition the XRF test was

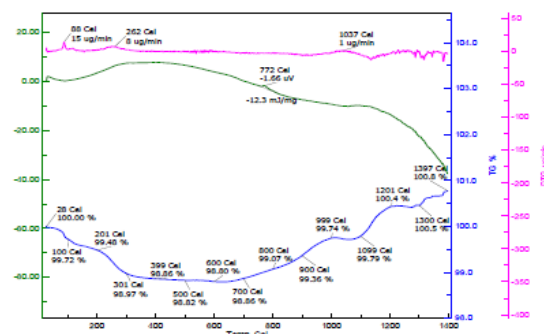


Figure 6 DTA, TG, DTG analysis of flux 1

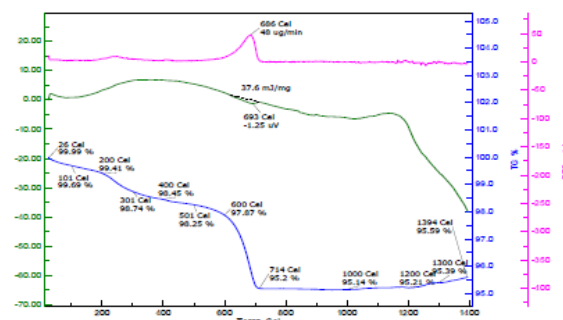


Figure 7 DTA, TG, DTG analysis of Commercial flux 1

performed. It is a non-destructive analytical technique. It determines the chemistry of a sample by measuring the fluorescent X-ray emitted from a sample when it is excited by a primary X-ray source. The result of the analysis is shown in the Table 7. In most of the fluxes, it has been observed that the SiO<sub>2</sub>, CaO, Al<sub>2</sub>O<sub>3</sub>, MgO, NiO and Na<sub>2</sub>O were present with the decreasing order of their weight percentage. Calcium was also present which increases the stability of electric arc during welding. The viscosity of fluxes increases by the presence of corundum and SiO<sub>2</sub> that too was also present in most of the fluxes. If we compare all the fluxes with the commercial flux the order of weight percentage is Al<sub>2</sub>O<sub>3</sub>, MnO, SiO<sub>2</sub>, CaO, Fe<sub>2</sub>O<sub>3</sub>, TiO<sub>2</sub>, MgO, Na<sub>2</sub>O and NiO slightly different from the designed flux.

#### IV. CONCLUSION

This study helped us to see the different crystalline phases present in the flux system along with the crystal systems because of different ions present in the developed fluxes. It helped in identifying the most reactive component that will either be absorbed in slag or retained in the weld as an inclusion. It also helped to study the effect of these oxides on the mechanical

strength of the weld. It helped to understand how the composition of flux affects the behaviour of weld metal in the weld pool due to various chemical reactions taking place. Melting behaviour and weight loss during

the analysis of all the fluxes is well explained by DTG and TG analysis. It is also explained that with the slight variation in the composition of the flux its behaviour also changes.

Table 6 TG Analysis of SiO<sub>2</sub> fluxes

	Type of flux									
	111	122	133	212	223	231	313	321	332	Comm. Flux
Temperature, Celsius	% Weight Loss									
26	99.99	99.98	99.98	99.98	99.98	99.99	99.99	99.99	99.99	100
101	99.69	99.49	99.53	99.52	99.48	99.17	99.55	99.22	99.66	99.71
200	98.41	99.01	99.08	99.40	98.98	98.35	99.21	98.46	99.29	99.48
301	98.74	98.32	98.28	98.38	98.31	97.57	98.65	97.18	98.5	98.97
400	98.45	97.99	97.79	97.55	97.99	97.18	98.37	96.4	98.2	98.86
501	98.25	97.76	97.57	97.02	97.74	96.87	98.12	96.07	98.07	98.82
600	97.87	97.26	97.1	96.83	97.17	96.24	97.6	95.51	97.74	98.86
714	95.2	93.1	93.4	95.1	93.9	91.7	94.3	91.1	96.4	99.07
1000	95.14	92.89	93.23	93.11	93.94	91.29	94.16	91.29	96.31	99.74
1200	95.21	92.94	93.23	93.20	93.92	91.05	94.14	91.44	96.2	100.4
1300	95.39	93.05	93.52	93.57	94.15	91.1	94.36	91.6	96.41	100.5

Table 7 XRF Analysis of SiO<sub>2</sub> fluxes

Flux	Na <sub>2</sub> O%	MgO%	Al <sub>2</sub> O <sub>3</sub> %	SiO <sub>2</sub> %	CaO%	TiO <sub>2</sub> %	MnO%	Fe <sub>2</sub> O <sub>3</sub> %	NiO%
1	2.30	2.54	6.22	32.0	17.8	0.2	0.83	0.58	1.93
2	1.47	2.02	3.2	25.2	15.5	326 PPM	1.16	0.71	2.10
3	2.29	2.80	6.45	32.2	16.9	0.13	1.01	1.14	2.62
4	1.62	2.27	4.19	26.6	16.7	0.34	1.23	0.94	2.63
5	0.47	3.08	4.64	32.9	17.8	571 PPM	1.53	1.05	2.35
6	1.98	2.17	5.35	28.0	16.8	615 PPM	0.81	0.90	2.92
7	0.26	2.44	4.56	28.8	17.7	571 PPM	1.12	0.88	3.05
8	0.17	1.62	4.81	18.7	14.0	0.44	1.41	1.11	2.9
9	2.1	2.2	4.56	26.6	16.8	0.80	1.66	1.53	2.99
Co. flux	1.96	2.18	15.40	7.7	7.17	3.94	11.10	5.07	475 PPM

## REFERENCES

- [1] Jackson, C.E., "Submerged arc welding, fluxes and relations among process variables in metals" hand book, ASM, Metals Park, OH, pp.73-77.
- [2] Indacochea, J.E., Blander, M., Shah .S. "Submerged arc welding, evidence for electrochemical effects on the weld pool", Weld. J. Supp. Res., 68(3), pp.77-79, 1989.
- [3] Wittstock, G.G., "Selecting submerged arc welding fluxes for carbon and low alloy steels", Welding Journal, pp.773-741, 1976.
- [4] Paniagua, M., Ana, M., Lopez, H., Victor, M., Munoz, M.L. "Influence of the chemical composition of flux on the microstructure and tensile properties of submerged-arc welds", Journal of Material processing technology, 169, PP.93-100, 2005.
- [5] Kanjilal, P., Pal, T.K., Majumdar, S.K., "Combined effect of flux and welding parameters on chemical composition and mechanical properties of Submerged arc weld metal", Journal of Materials processing technology, 171, pp.223-231, 2006.
- [6] Allen, A.W. "Optical microscopy in ceramic engineering", Proceedings of the third Berkely International Materials conference, Berkely, CA, June 1966.
- [7] Singer S.S., Industrial Ceramics, Chapman & Hall, London, pp.236-257, 1963.
- [8] Redwine, R.H., Concord, M.A., "Microstructures developed in crystallized glass ceramics", Proceedings of the third Berkely International Materials conference, Berkely, CA, June 1961.
- [9] Paniagua, A. M, Estrada, D., Lopez, H., Victor, M., "Chemical and structural characterization of the crystalline phases in agglomerated flux for submerged-arc welding", Journal of Material processing technology, 141, pp.93-100, 2003.

- [10] Dunham, W.B., Christian, A., "Process Mineralogy of Ceramic Materials", Elsevier, New York, pp. 20-48, 1984.
- [11] Arnulf, M., Osborn, E.F., "Phase equilibrium among oxides in steel making, Addison-Wesley, USA, 1965.

